Accurate Representation of Light-intensity Information by the Neural Activities of Independently Firing Retinal Ganglion Cells

Sang Baek Ryu[1,3], Jang Hee Ye[2,3], Chi Hyun Kim[1], Yong Sook Goo[2,3], and Kyung Hwan Kim[1,3]

[1]Department of Biomedical Engineering, College of Health Science, Yonsei University, Wonju 220-710, [2]Department of Physiology, Chungbuk National University School of Medicine, Cheongju 361-763, [3]Nano Artificial Vision Research Center, Seoul National University Hospital, Seoul 110-744, Korea

For successful restoration of visual function by a visual neural prosthesis such as retinal implant, electrical stimulation should evoke neural responses so that the information on visual input is properly represented. A stimulation strategy, which means a method for generating stimulation waveforms based on visual input, should be developed for this purpose. We proposed to use the decoding of visual input from retinal ganglion cell (RGC) responses for the evaluation of stimulus encoding strategy. This is based on the assumption that reliable encoding of visual information in RGC responses is required to enable successful visual perception. The main purpose of this study was to determine the influence of inter-dependence among stimulated RGCs activities on decoding accuracy. Light intensity variations were decoded from multiunit RGC spike trains using an optimal linear filter. More accurate decoding was possible when different types of RGCs were used together as input. Decoding accuracy was enhanced with independently firing RGCs compared to synchronously firing RGCs. This implies that stimulation of independently-firing RGCs and RGCs of different types may be beneficial for visual function restoration by retinal prosthesis.

Key Words: Retinal prosthesis, Retinal ganglion cell, Multielectrode arrray (MEA), Optimal linear filter, Spike train decoding, Functional connectivity

INTRODUCTION

Retinal diseases such as retinitis pigmentosa and age-related macular degeneration induce gradual loss of vision, which can eventually lead to total blindness. A significant number of retinal ganglion cells (RGCs) forming the optic nerve, however, are often morphologically intact and remain functionally viable (Santos et al., 1997). The visual neural prosthesis, such as a retinal prosthesis, may be able to restore visual function by using electrical pulses to stimulate RGCs to transmit visual information to the brain (Majji et al., 1999; Zrenner, 2002; Humayun et al., 2003; Rizzo et al., 2003; Merabet et al., 2005).

For successful restoration of vision, the neural activities of electrically stimulated RGCs should contain information on spatial and temporal patterns of incoming visual input. Thus, it is necessary to determine how to generate electrical stimulation for effective sensory information transmission, just as the case of cochlear implant. We refer to the method of generating electrical stimulation based on the sensory input as encoding strategy. Quantitative information on incoming visual input can be reconstructed or 'decoded' from

the neural activities of RGCs by spike train decoding algorithms (Warland et al., 1997; Nicolelis, 1998). Using spike train decoding, it may also be possible to evaluate the effectiveness of stimulus encoding strategies by comparing the actual and estimated input reconstructed from RGC responses, since a better encoding strategy should provide more reliable transmission of information on input stimuli. Recently, we established a method for the reconstruction of light intensity variation from multiple RGC responses, as a preliminary study for the evaluation of encoding strategy (Ryu et al., 2007).

In this paper, we investigated the influences of inter-dependence among the activities of RGCs and types of RGCs on the accuracy of decoding visual input. We compared the accuracies of light intensity decoding when the group of RGCs showed independently-firing or synchronously-firing characteristics. Inter-dependence among RGC activities was identified based on the ensemble response characteristics to light stimulus (Meister et al., 1995). Usually, nearby cells and the cells with the same firing property showed synchronously firing characteristics, and cells of different types showed independently firing patterns. We used each RGC group separately as the input of the decoding algorithm to reconstruct the light intensity variation, and compared the reconstruction accuracy for various light stimuli.

ABBREVIATIONS: RGC, retinal ganglion cell; MEA, multi-electrode array; PSTH, post-stimulus time histogram.

METHODS

Details on experimental methods were previously described (Cho et al., 2004). Retinas from two dark-adapted New Zealand white rabbits (male, weight: ~2 kg) were isolated after anesthesia. All animal use protocols were approved by the institutional animal care committee of Chungbuk National University (permission number: CA-25). Four patches of retina (near the center of visual field) were detached and cut to ~5×5 mm and attached to a planar multielectrode array (MEA, Multichannel systems GmbH, Germany), so that the retinal ganglion cell layer faced the electrodes. The MEA contains 60 circular TiN electrodes with 200 μm interelectrode spacing. The radii of electrodes were 30 μm, and impedances were about 50 kΩ at 1 kHz. The MEA 60 recording system (Multichannel systems GmbH, Germany) was used for data acquisition. The data acquisition system consists of a RS-232 interface for the synchronization of stimulus and recording, an integrated 60-channel preamplifier and a bandpass filter system (MEA 1060, amplification gain: 1200, passband: 10~3,000 Hz), and a PC. Raw data from the MEA were recorded with a sampling rate of 25 kHz/channel, stored using data acquisition software (MC_Rack, Multichannel systems GmbH, Germany), and transformed into single unit spike trains by a spike extraction program (Offline Sorter, Plexon inc., TX, USA). In most cases, each electrode contained activities from only one RGC, although spike sorting was also performed. When it was difficult to sort spikes from a single-unit RGC due to spike overlap problem, we did not include the data from that RGC in data pool for further analysis.

Continuously-modulated light was generated by a PC monitor, and then uniformly presented onto the MEA by a LCD beam projector and an inverted microscope (Nikon Diaphot, Japan). Stimulus presentation software, PRE-SENTATION (Neurobehavioral Systems Inc., USA), was used for the generation of light intensity variation. The maximum light intensity was 1.37 μW/cm^2. Two types of light intensity modulation were adopted: 1) ON-OFF stimulus: repetition of 2 s on (i.e., highest brightness of the PC monitor) and 5 s off (i.e., lowest brightness of the PC monitor) periods, 2) Gaussian random stimulus: random intensity variation following Gaussian distribution (mean:

70% of maximum intensity, std.: 3% of the mean intensity). The frame rate of the random stimulus presentation was changed from 1 to 8 Hz to examine the effect of the rate of light intensity variation on decoding accuracy. The time courses of light intensities are shown in Fig. 1 along with the reconstructed waveforms obtained from spike train decoding.

The types of RGCs were identified from response characteristics to repetitive ON-OFF stimulus, based on inspection of post stimulus time histograms (PSTH) (Nicolelis, 1998). A simple criterion was used to classify the RGCs into three groups; ON, OFF, and ON-OFF cells. If an RGC showed a rapid increase in firing rate immediately after the application of ON stimulus, it was classified as an ON cell. If an RGC showed response characteristics opposite to this, it was classified as an OFF cell. The ON-OFF cell actively responded to both the onset and cessation of light. All the RGCs analyzed showed transient, rather than sustained, response characteristics.

To find the groups of RGCs with independently or synchronously firing characteristics, a cross-correlation analysis of spontaneous activities was performed (Ye et al., 2008). We used cross-correlogram, which is a standard method of estimating the degree to which two spike trains are correlated. It is a histogram that shows how the spikes from a target cell are distributed in time with respect to the spikes from a reference cell (Nicolelis, 1998). Examples of cross-correlogram are shown in Fig. 2 ((A): two synchronously firing cells, (B): two independently firing cells). If there is an evident peak in the cross-correlogram as the two cases shown in Fig. 2A, it is defined that the two cells are synchronously-firing cells. When there is no conspicuous peak in the cross-correlogram as the two cases shown in Fig. 2B, they are regarded as two independently-firing cells. Based on this, we formed cell groups consisting of three RGCs for the comparison of the independently-firing and synchronously-firing RGC groups. First, one RGC was chosen as a reference cell. Two cells showing strong correlation with the reference cell were selected. If these two cells showed strong correlation with each other also, they and the reference cell were collected as synchronously firing cell group. A strong correlation was defined as the peak amplitude of the cross-correlogram being higher than 4 spikes/bin, and
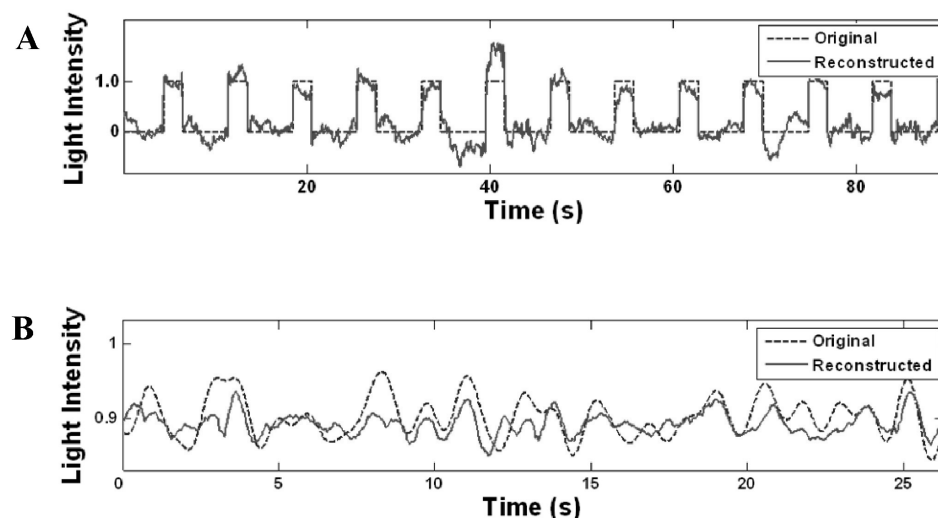

Fig. 1. Temporal patterns of light stimulus intensity variation. Dotted: original stimulus, Solid: reconstructed stimulus by spike train decoding. (A) ON-OFF stimulus (ON: 2 s, OFF: 5 s, decoding from 4 ON RGCs), (B) Gaussian random stimulus (decoding from 5 ON RGCs). The light intensity (y axis) is represented with respect to the minimum and maximum intensity ('0' and '1' denote the minimum and the maximum intensity levels, respectively). Frame rate was 1 Hz.
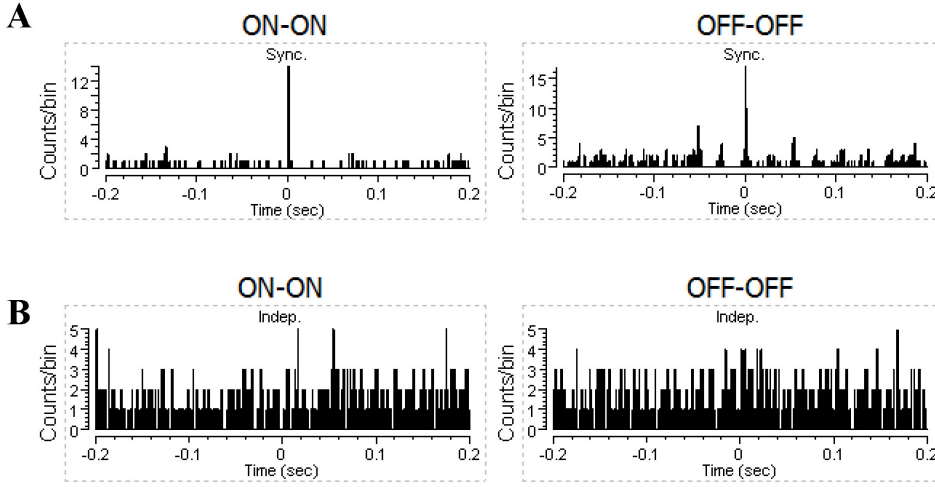
A

B

Fig. 2. Examples of cross-correlograms for two synchronously-firing (A), and independently-firing (B) RGCs.
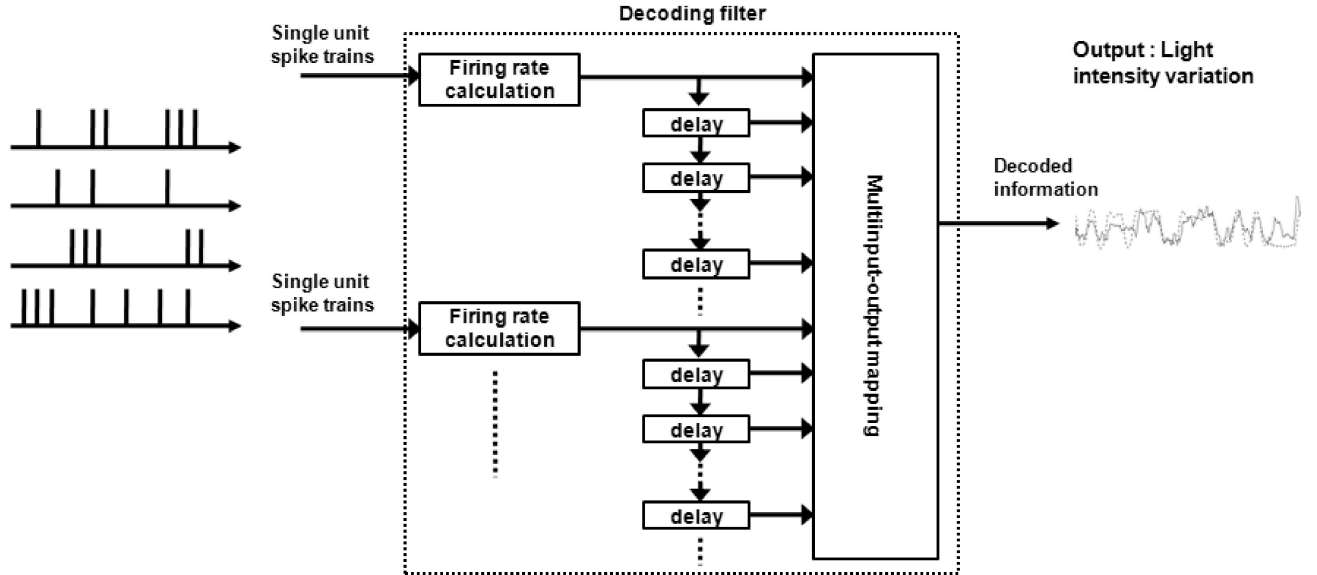

Fig. 3. Structure of an optimal linear decoding filter for multiple RGC spike trains.

the width of the peak being smaller than 10 ms ($-5 \sim +5$ ms from the center). Similar grouping was performed to form independently firing RGC groups by selecting two cells that showed no correlation between each other, as well as with the reference cell.

Spike train decoding is a procedure to reconstruct, or to 'decode' quantitative information encoded in the neural responses (spike train). Here we used an optimal linear filter for spike train decoding (Kim et al., 2006). From the time series of light intensity variation and RGC spike train responses, the coefficients of an optimal linear filter can be obtained by the least squares method (Kim et al., 2006). The structure of this decoding filter is illustrated in Fig. 3. Here the visual input, i.e. light intensity, is estimated from multiunit RGC firing rates by linear regression.

Spike trains were transformed into firing rate time series by counting the number of spikes within 50 ms time bins.

The time series of firing rate and stimulus waveform are represented as matrices R and s as explained below to obtain the filter coefficients by the least squares method, which determine the linear mapping of Fig. 3. The matrix R consists of multiple RGC responses and is expressed as follows:

$$\mathbf{R} = \begin{bmatrix} 1 & r_1(0) & r_1(1) & \cdots & r_1(M-1) & \cdots & r_N(0) & \cdots & r_N(M-1) \\ 1 & r_1(1) & r_1(2) & \cdots & r_1(M) & \cdots & r_N(1) & \cdots & r_N(M) \\ 1 & \cdots & \cdots & \cdots & \cdots & \cdots & \cdots & \cdots & \cdots \\ 1 & r_1(L) & r_1(L+1) & \cdots & r_1(L+M-1) & \cdots & r_N(L) & \cdots & r_N(L-M+1) \end{bmatrix} \quad (1)$$

Here $r_p(i)$ is the firing rate of the pth unit in the ith time bin and the length of time bin was fixed at 50 ms. L denotes the length of the training data. M and N are the number of filter taps (i.e., the number of delay elements in Fig. 3), and the number of units, respectively. s is a vector repre-

senting the true stimulus (i.e. light intensity variation) and can be written as:

$$\mathbf{s} = [s(0)\ s(1)\ \cdots\ s(L\text{-}1)]^T \qquad (2)$$

The coefficients of this filter, f, are obtained by the least-squares methods as follows (Warland et al., 1997; Kim et al., 2006)

$$\mathbf{f} = (\mathbf{R}^T\mathbf{R})^{-1} \cdot (\mathbf{R}^T\mathbf{s}) \qquad (3)$$

where,

$$\mathbf{f} = [f_1(0)\ f_1(1)\cdots f_1(M-1)\ \cdots\ f_p(0)\cdots\ f_p(M\text{-}1)]^T \quad (4)$$

Here, $f_p(j)$ corresponds to the jth coefficient of the linear filter whose input is the firing rates of the pth RGC. From

available recordings, the first half of the data was used for training the decoding filter, i.e. for the calculation of filter coefficients, and the other half was used for the reconstruction. Once the filter coefficients were obtained, the light stimulus intensity was reconstructed or 'decoded' as follows:

$$u(i) = \sum_{p=1}^{N}\sum_{j=0}^{M-1} r_p(i-j)f_p(j) \qquad (5)$$

Here, $u(i)$ is the estimated value of input stimulus at the ith time bin. The accuracy of decoding can be quantified by the similarity between the original and decoded light intensity waveforms. Thus, to measure the similarity which provides the index of decoding accuracy, we calculated the correlation coefficient between the two waveforms, as did Wessberg et al. (2000).
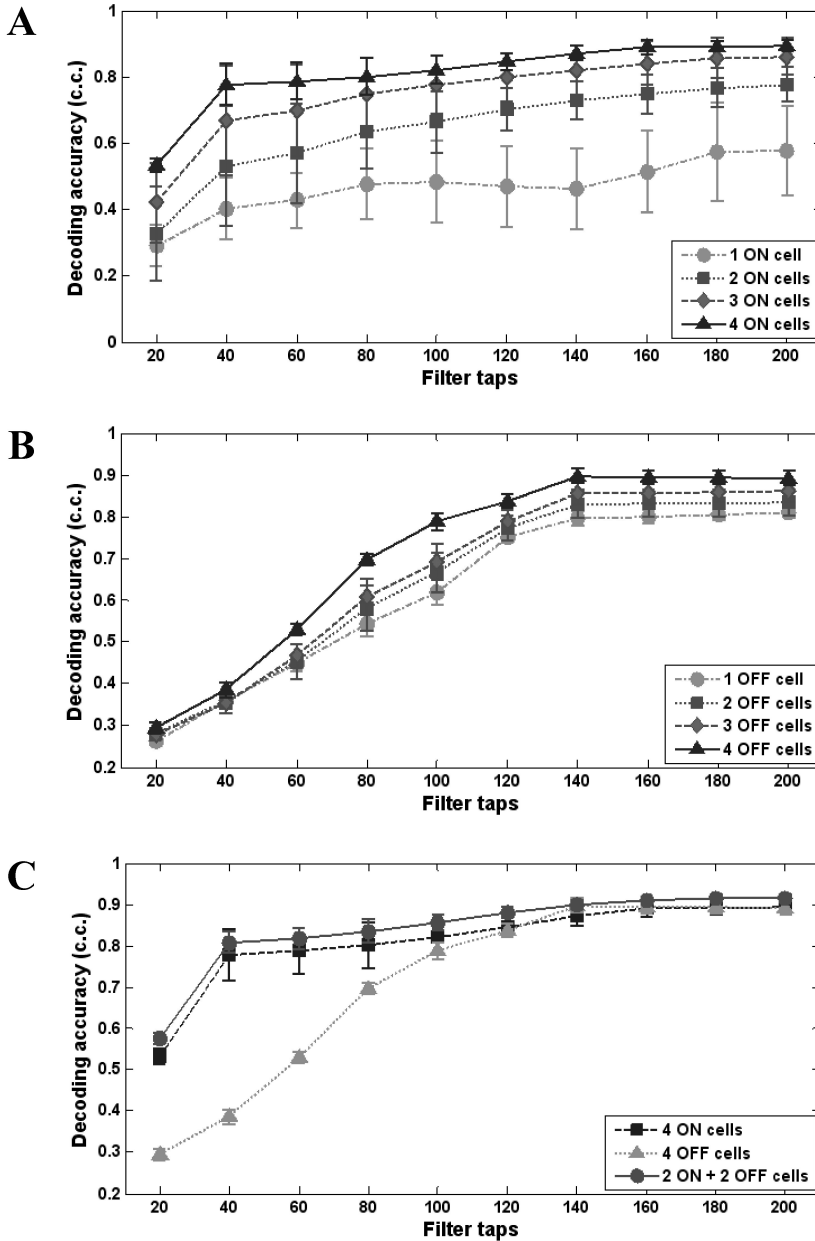

Fig. 4. Variation of the decoding accuracy as a function of the number of filter taps. (A) ON cells (1~4 cells), (B) OFF cells (1~4 cells), (C) 2 ON cells and 2 OFF cells used together for the decoding. Each data point was obtained from 3 repeated trials of decoding from 100 s data. Error bars denote standard error.
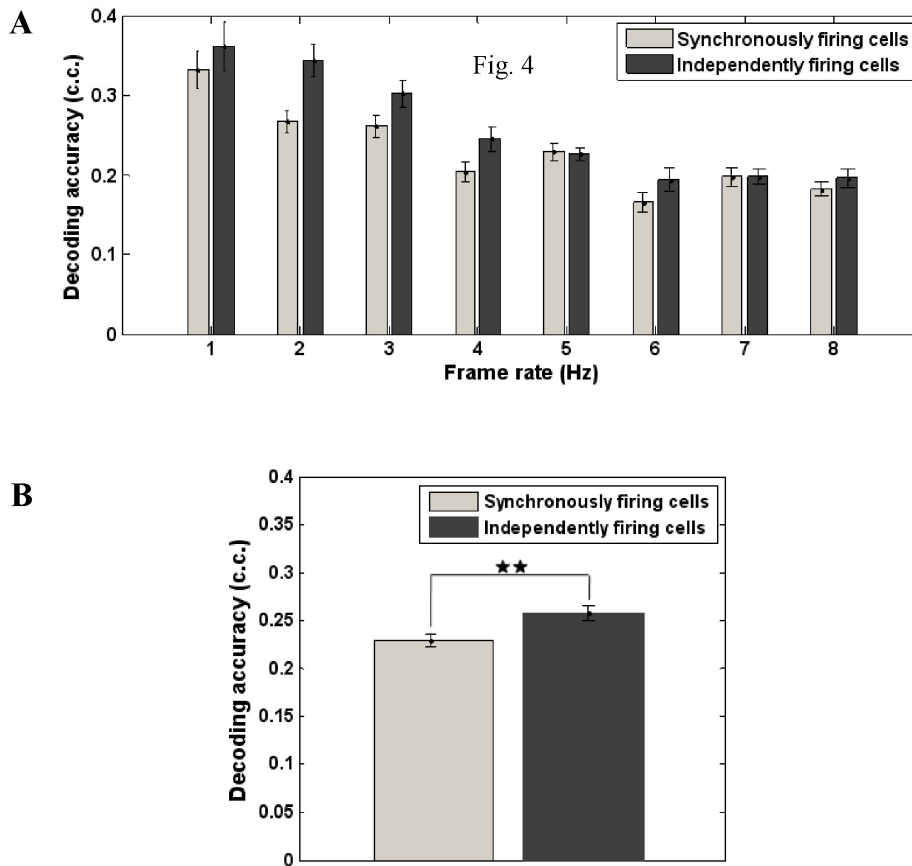
A

Fig. 4

B

Fig. 5. (A) Variation of the decoding accuracy as a function of frame rate, for Gaussian random stimuli obtained from 21 repeated trials (3 trials×7 cell groups), (B) Comparison of the decoding results of synchronously- firing and independently-firing RGCs, for Gaussian random stimuli (8 stimuli× 3 trials×7 cell groups).

RESULTS

Neural activities from 75 RGCs could be reliably identified from four retinas (average number of RGCs per patch: 18.75 ± 7.67). Typical results of reconstructed light intensity waveforms obtained from spike train decoding are shown in Fig. 1, along with original ones. Fig. 4 shows the correlation between the actual and decoded ON-OFF stimuli as a function of the number of filter taps, M. Each data point in Fig. 4 was obtained from 3 repeated trials of decoding from 100 s data. The errorbars denote standard error. The increase in decoding accuracy was saturated at $100 \sim 140$ filter taps. Regardless of the cell type, the correlation between actual and reconstructed stimuli increased and became saturated as more cells were employed (Fig. 4A, B). Furthermore, more accurate decoding was possible when both ON and OFF cells were used together (Fig. 4C). When both ON and OFF cells were adopted, further increase of decoding accuracy was observed up to about 10 cells (not shown). This result implies that more reliable transmission of visual information is feasible when different types of RGCs are simultaneously stimulated.

Significant differences were observed in decoding accuracies for 4 ON cells compared to 2 ON cells+2 OFF cells (t-test, p=0.0294). These results imply that more reliable transmission of visual information is feasible when different types of RGCs are simultaneously stimulated. Also from the comparison of 4 OFF cells and 2 ON cells+2 OFF cells, we could observe statistically significant difference (t-test, p=0.0242).

To compare the decoding accuracies between the cases of adopting independently- and synchronously-firing cell groups, seven RGCs groups were identified for each case. More accurate decoding was possible for independently-firing RGC groups, compared to synchronously-firing groups. Fig. 5 shows the decoding results for Gaussian random stimuli obtained from 21 repeated trials per each frame rate (3 trials×7 cell groups) of decoding from 30 s data at various frame rates which cause the change of the rate of light intensity variation. As shown in Fig. 5 the decoding accuracy was generally higher when independently-firing cell groups were used for spike train decoding, at all frame rates. Statistical comparison showed that the correlation coefficient between the actual and reconstructed stimuli was larger when independently-firing RGC groups were adopted for decoding, compared to the case of using synchronously-firing groups, and this was nearly statistically significant (t-test, $p < 0.001$).

DISCUSSION

For successful restoration of impaired visual function by visual neural prosthesis such as a retinal implant, it is necessary to determine how to generate electrical stimulation for reliable transmission of visual information (Stett et al., 2000; Sekirnjak et al., 2006). We suggest decoding of visual input information from RGC responses as a method for evaluating the effectiveness of the stimulus encoding strategy. In this paper, we performed a first-round study

using light stimulation instead of electrical stimulation, and focused on the investigation of influence of the types of RGCs and correlation among RGCs on the light intensity decoding accuracy. Light stimuli intensity variations were estimated using an optimal linear filter obtained from given stimulus intensity variation and multiple single unit spike trains from RGCs. The decoding accuracy depended on RGC type and their inter-dependence. More exact decoding was possible when different RGC types were used together, and when the independently-firing RGC groups were used, compared to synchronously firing groups.

It can be stated that successful perception of visual information by electrical stimulation of retinal implant is expected when sufficient information on visual input is properly encoded within the neural responses of RGCs evoked by stimulation. Thus, better restoration of visual function is possible when we can more accurately decode the information on visual input from the RGC spike trains. Although visual information is perceived in the brain, the minimization of information loss at the transmission site (i.e., retina) should be a prerequisite for successful information retrieval at the receiving site (i.e., the brain). From spike train decoding, the accuracy of information transfer can be quantified, and a quantitative index on the effectiveness of stimulus encoding strategy can be obtained.

More accurate decoding was possible as more cell activity is used as to decode the input. The accuracy of decoding simple ON-OFF intensity variation became saturated when it was decoded from more than four cells if they were of same type. However, the use of both ON and OFF cells further increased performance. From this result, we infer that cells with different types (ON cells and OFF cells) convey independent information so that simultaneous stimulation of them may result in superior decoding accuracy. We used simple criteria for RGC classification, but further detailed criteria should be adopted for a more comprehensive study on how RGC types affect decoding accuracy. Thorough characterization of the spatiotemporal receptive field of RGCs may be helpful for this purpose (Brown et al., 2000).

The investigation of the effects of interdependence among the RGC activities on the accuracy of spike train decoding revealed that stimulations of independently-firing cell groups and RGCs of different types are more advantageous for reliable transmission of visual information to the brain. From this, we infer that superior perception of visual information may be obtained by stimulating independently firing RGC groups and the RGCs of different types, when retinal implants would be implemented. Two independently firing neurons may convey independent information on input, whereas two neurons with closely correlated firing characteristics may carry redundant information. Thus it is plausible that more exact decoding is expected from the independently-firing RGC groups.

This preliminary postulation should be tested further. We only considered the encoding of temporal in this study. Further study is necessary for the consideration of spatial information as well as temporal information. For the development of the encoding strategies for electrical stimulation pulse generation in retinal implants, studies of electrically stimulated RGC responses are necessary. Modulations of stimulus amplitude, duration, and pulse rate are candidates for the modulation when encoding external visual information into electrical pulse trains, and thus, the decoding accuracy should be investigated while changing these parameters.

Many techniques have been recently proposed for spike train decoding (Brown et al., 2004) and more complicated algorithms may be used such as multilayer neural networks (Warland et al., 1997). However, the optimal linear filter is advantageous in that a unique solution for the given training data is obtained by a closed-form equation. The use of iterative learning does not give identical solutions for each training session. As suggested by Field and Chichilnisky (2007), a better model of the nature of visual stimulus encoding in the retina may help obtain an optimal decoding method.

ACKNOWLEDGEMENTS

REFERENCES

Brown EN, Kass RE, Mitra PP. Multiple neural spike train data analysis: state-of-the-art and future challenges. *Nat Neurosci* 7: 456−461, 2004.

Brown SP, He S, Masland RH. Receptive field microstructure and dendritic geometry of retinal ganglion cells. *Neuron* 27: 371−383, 2000.

Cho HS, Jin GH, Goo YS. Characterization of rabbit retinal ganglion cells with multichannel recording. *Korean J Med Phys* 15: 228−236, 2004.

Field GD, Chichilnisky EJ. Information processing in the primate retina: circuitry and coding. *Annu Rev Neurosci* 30: 1−30, 2007.

Fried SI, Hsueh HA, Werblin FS. A method for generating precise temporal patterns of retinal spiking using prosthetic stimulation. *J Neurophysiol* 95: 970−978, 2006.

Humayun MS, Weiland JD, Fujii GY, Greenberg R, Williamson R, Little J, Mech B, Cimmarusti V, Boemel GV, Dagnelie G, de Juan E. Visual perception in a blind subject with a chronic microelectronic retinal prosthesis. *Vision Res* 43: 2573−2581, 2003.

Kim KH, Kim SS, Kim SJ. Superiority of nonlinear mapping in decoding multiple single-unit neuronal spike trains: a simulation study. *J Neurosci Methods* 150: 202−211, 2006.

Majji AB, Humayun MS, Weiland JD, Suzuki S, D'Anna SA, de Juan E. Long-term histological and electrophysiological results of an inactive epiretinal electrode array implantation in dogs. *Invest Ophthalmol Vis Sci* 40: 2073−2081, 1999.

Meister M, Lagnado L, Baylor DA. Concerted signaling by retinal ganglion cells. *Science* 270: 1207−1210, 1995.

Merabet LB, Rizzo JF, Amedi A, Somers DC, Pascual-Leone A. What blindness can tell us about seeing again: merging neuroplasticity and neuroprosthesis. *Nat Rev Neurosci* 6: 71−77, 2005.

Nicolelis MAL. Methods for Neural Ensemble recording. CRC Press, Florida, 1998.

Rizzo JF, Wyatt J, Loewenstein J, Kelly S, Shire D. Methods and perceptual thresholds for short-term electrical stimulation of human retina with microelectrode arrays. *Invest Ophthalmol Vis Sci* 44: 5355−5361, 2003.

Ryu SB, Kim DH, Ye JH, Kim KH, Goo YS. Estimation of visual stimulus intensity from retinal ganglion cell spike trains using optimal linear filter. *J Biomed Eng Res* 28: 212−217, 2007.

Santos A, Humayun MS, de Juan E, Greenburg RJ, Marsh MJ, Klock IB, Milam AM. Preservation of the inner retina in retinitis pigmentosa: *a morphometric analysis. Arch Ophthal* 115: 511−515, 1997.

Sekirnjak C, Hottowy P, Sher A, Dabrowski W, Litke AM,

Chichilnisky EJ. Electrical stimulation of mammalian retinal ganglion cells with multielectrode array. *J Neurophysiol* 95: 3311−3327, 2006.

Stett A, Barth W, Weiss S, Haemmerle H, Zrenner E. Electrical multisite stimulation of the isolated chicken retina. *Vision Res* 40: 1785−1795, 2000.

Warland DK, Reinagel P, Meister M. Decoding visual information from a population of retinal ganglion cells. *J Neurophysiol* 78: 2336−2350, 1997.

Wessberg J, Stambaugh CR, Kralik JD, Beck PD, Laubach M, Chapin JK, Kim J, Biggs SJ, Srinivasan MA, Nicolelis MA. Real-time prediction of hand trajectory by ensembles of cortical neurons in primates. *Nature* 408: 361−365, 2000.

Ye JH, Ryu SB, Kim KH, Goo YS. Functional connectivity map of retinal ganglion cells for retinal prosthesis. *Korean J Physiol Pharmacol* 12: 307−314, 2008.

Zrenner E. Will retinal implants restore vision? *Science* 295: 1022−1025, 2002.